

A note on the lack of symmetry in the graphical lasso

Benjamin T. Rolfs^{a,*}, Bala Rajaratnam^b

^a*Inst. for Computational and Applied Mathematics, Stanford University, Stanford, CA 94395*

^b*Department of Statistics, Stanford University, Stanford, CA 94305*

Abstract

The graphical lasso (glasso) is a widely-used fast algorithm for estimating sparse inverse covariance matrices. The glasso solves an ℓ_1 penalized maximum likelihood problem and is available as an R library on CRAN. The output from the glasso, a regularized covariance matrix estimate $\hat{\Sigma}_{glasso}$ and a sparse inverse covariance matrix estimate $\hat{\Omega}_{glasso}$, not only identify a graphical model but can also serve as intermediate inputs into multivariate procedures such as PCA, LDA, MANOVA, and others. The glasso indeed produces a covariance matrix estimate $\hat{\Sigma}_{glasso}$ which solves the ℓ_1 penalized optimization problem in a dual sense; however, the method for producing $\hat{\Omega}_{glasso}$ after this optimization is inexact and may produce asymmetric estimates. This problem is exacerbated when the amount of ℓ_1 regularization that is applied is small, which in turn is more likely to occur if the true underlying inverse covariance matrix is not sparse. The lack of symmetry can potentially have consequences. First, it implies that $\hat{\Sigma}_{glasso}^{-1} \neq \hat{\Omega}_{glasso}$ and second, asymmetry can possibly lead to negative or complex eigenvalues, rendering many multivariate procedures which may depend on $\hat{\Omega}_{glasso}$ unusable. We demonstrate this problem, explain its causes, and propose possible remedies.

Keywords: Concentration model selection, glasso, Graphical Gaussian Models, graphical lasso, ℓ_1 regularization.

1. Introduction

In modern applications, many data sets are simultaneously high-dimensional and low in sample size. Classic examples include microarray gene expression and SNP data. Dealing with such datasets has become an area of great interest in many fields such as biostatistics. Algorithms such as the graphical lasso (Friedman et al., 2008; Hastie et al., 2009) have been proposed to obtain regularized covariance estimators in the $n \ll p$ setting (where n is the sample size and p is the problem dimension) as well as perform graphical model selection.

In the case of the graphical lasso, graphical model selection involves inferring a concentration graph (or equivalently, a Markov model). A concentration graph encodes zeros in the inverse covariance (concentration) matrix, i.e., $i \not\sim j$ for $i, j \in \{1, \dots, p\}$ in the graph implies that the partial correlation $\rho(X_i, X_j | X_{k \notin \{i, j\}}) = 0$. Along with inferring such a graph, the glasso provides $p \times p$ dimensional matrix

*Corresponding author

Email addresses: benrolfs@stanford.edu (Benjamin T. Rolfs), brajarat@stanford.edu (Bala Rajaratnam)

estimators for both the covariance and concentration matrices, denoted $\hat{\Sigma}_\lambda$ and $\hat{\Omega}_\lambda$ respectively, for a given penalty parameter $\lambda > 0$. In particular, $\hat{\Omega}_\lambda$ is the solution to the convex maximization problem

$$\hat{\Omega}_\lambda = \hat{\Sigma}_\lambda^{-1} = \arg \min_{X \succ 0} [\log \det (X) - \text{tr} (SX) - \lambda \|X\|_1] \quad (1)$$

where S is the sample covariance matrix, $X = \{x_{ij}\}_{i,j=1}^p$ is positive definite and $\|X\|_1 = \sum_{i,j} |x_{ij}|$. The non-zero elements of $\hat{\Omega}_\lambda$ correspond to edges in the estimated concentration graph.

In some applications, graphical model selection is the primary goal, where in other situations the estimators $\hat{\Sigma}_\lambda$ and $\hat{\Omega}_\lambda$ are used as inputs into other multivariate algorithms where a regularized covariance estimator is required. Typical examples include LDA, PCA, and MANOVA. Hence, it is often necessary that not only $\hat{\Sigma}_\lambda^T = \hat{\Sigma}_\lambda \succ 0$, but also that $\hat{\Omega}_\lambda^T = \hat{\Omega}_\lambda$, $\hat{\Omega}_\lambda \succ 0$, and $\hat{\Omega}_\lambda^{-1} = \hat{\Sigma}_\lambda$. We find that the output of the graphical lasso does not meet these conditions in certain situations, explain why, and discuss how to solve this problem. Such situations arise primarily when S is rank-deficient and λ is small. A low level of regularization is required when the true underlying concentration matrix is not sparse. It should however be noted that the glasso algorithm does indeed solve the dual problem corresponding to (1), so the above assertions should be interpreted in context.

2. Motivating Examples

We now present two motivating examples, one in a classical setting and another in a high-dimensional setting, to illustrate the problem.

2.1. Example 1: Low dimensional, large sample size inverse covariance estimation

Consider $n = 500$ *i.i.d.* samples drawn from a $p = 5$ dimensional multivariate Gaussian distribution with mean $\mu = 0$ and concentration matrix:

$$\Omega = \begin{bmatrix} 2.425 & 0.069 & -0.885 & 0 & 0 \\ 0.069 & 2.944 & -0.129 & 0.988 & 0 \\ -0.885 & -0.129 & 2.696 & 0.035 & -0.974 \\ 0 & 0.988 & 0.035 & 1.724 & 0.851 \\ 0 & 0 & -0.974 & 0.851 & 1.000 \end{bmatrix}$$

The glasso algorithm was applied to this data set. A regularization parameter of $\lambda = 0.0033$, which is close to the cross-validated estimate, was chosen to demonstrate the problem. The glasso estimators for Ω and $\Sigma = \Omega^{-1}$ for a given λ are denoted $\hat{\Omega}_\lambda$ and $\hat{\Sigma}_\lambda$.

For reasons which are clarified in Section 3, the glasso produces estimators which are neither symmetric nor true inverses of one another, i.e., $\hat{\Omega}_\lambda^T \neq \hat{\Omega}_\lambda$ and $\hat{\Sigma}_\lambda^{-1} \neq \hat{\Omega}_\lambda$. To quantify the lack of symmetry, consider the matrix of relative errors between the elements of $\hat{\Omega}_\lambda$ and $\hat{\Omega}_\lambda^T$, as defined by $Err_{ij} = 100 \left| \frac{\hat{\Omega}_\lambda(i,j) - \hat{\Omega}_\lambda^T(i,j)}{\hat{\Omega}_\lambda(i,j)} \right| \%$.

For the numerical example above,

$$Err = \begin{bmatrix} 0 & 1.94 & 0.05 & 0 & 0.25 \\ 1.98 & 0 & 2.84 & 0.04 & \infty \\ 0.05 & 2.77 & 0 & 0.88 & 0.04 \\ 0 & 0.04 & 0.89 & 0 & 0.01 \\ 0.25 & 100.00 & 0.04 & 0.01 & 0 \end{bmatrix}$$

with the convention that if $\hat{\Omega}_\lambda(i, j) = 0 = \hat{\Omega}_\lambda(j, i)$ then $Err_{ij} = 0$. Note that the entries $Err_{5,2} = 100\%$ and $Err_{2,5} = \infty$ occur because $\hat{\Omega}_\lambda(5, 2) \neq 0$ while $\hat{\Omega}_\lambda(2, 5) = 0$.

Although the relative errors are small, i.e., on the order of 2%, there is a clear lack of symmetry in $\hat{\Omega}_\lambda$ and moreover the sparsity patterns in the upper and lower parts of $\hat{\Omega}_\lambda$ are different, and thus yield two different graphical models. In particular, $\hat{\Omega}_\lambda(5, 2) \neq 0$ which indicates an edge between variables 2 and 5, while $\hat{\Omega}_\lambda(2, 5) = 0$ indicates the absence of such. Furthermore, in high-dimensional examples, a graph is often calculated automatically when $\left(\hat{\Omega}_\lambda\right)_{ij} > \epsilon$ for some small ϵ . In such cases, a lack of symmetry may result, yielding two separate graphs.

2.2. Example 2: High dimensional, low sample size autoregressive model

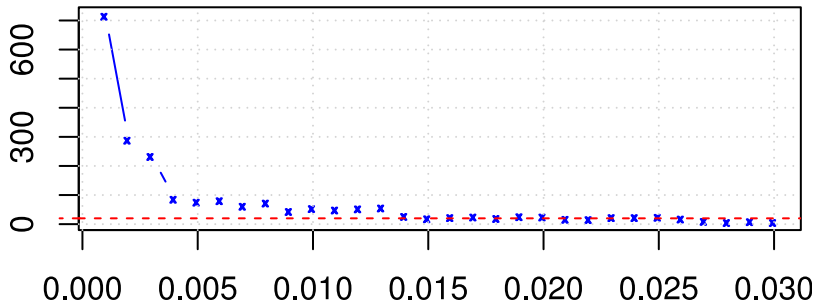
The lack of symmetry in $\hat{\Omega}_\lambda$, and the resulting difference in the concentration graphs corresponding to the upper and lower parts of $\hat{\Omega}_\lambda$, often becomes more pronounced as the dimension p grows.

We now consider a high dimensional example with $n = 250$ *i.i.d.* samples drawn from a Gaussian AR(1) model such that $X_{t+1} = \phi X_t + \epsilon_t$ for $t = 2, \dots, p$ and $X_1 = \epsilon_1$. Here, $p = 500$, $\phi = 0.75$, and $\epsilon_t \stackrel{i.i.d.}{\sim} \mathcal{N}(0, 1)$, $t = 1, \dots, p$. The concentration matrix Ω is tridiagonal, with the diagonal entries equal to 1 and the off-diagonal entries equal to -0.75 .

Given a glasso estimator $\hat{\Omega}_\lambda$, let E_1 and E_2 denote the edge sets corresponding to the upper and lower halves of $\hat{\Omega}_\lambda$, respectively. Then the symmetric difference $|E_1 \Delta E_2|$ is the number of edges which are present in the concentration graph encoded by one half of $\hat{\Omega}_\lambda$ but not in the graph encoded by the other half.

The glasso algorithm was applied to samples from the above model with the regularization parameter λ taking values between 0.001 and 0.03 in increments of 0.001. To put these values in perspective, note that when $\lambda = 0.03$, 102, 278 out of 124, 750 (82%) of the estimated off-diagonal entries were 0. The number of edge differences $|E_1 \Delta E_2|$ corresponding to $\hat{\Omega}_\lambda$ as λ varies between 0.001 and 0.03 is shown in Figure 1.

Figure 1: $|E_1 \Delta E_2|$ vs. λ for an AR(1) model with $\phi = 0.75$, $p = 500$, and $n = 250$. The red dashed line is at $|E_1 \Delta E_2| = 20$.



Note that at small values of λ , the difference in the graphs corresponding to the upper and lower parts of $\hat{\Omega}_\lambda$ as denoted by $|E_1 \Delta E_2|$ can be substantial. Hence,

the lack of symmetry in $\hat{\Omega}_\lambda$ can result in two completely different graphical models. Moreover, although $|E_1 \Delta E_2|$ decreases as λ increases it nevertheless remains nonzero as regularization increases.

2.3. Consequences of asymmetry in the glasso concentration matrix estimator

Users of the glasso may find the lack of symmetry a problem for a number of reasons:

1. $\hat{\Omega}_\lambda$ is not a mathematically valid estimator for $\hat{\Omega}$, since $\hat{\Omega}_\lambda^T \neq \hat{\Omega}_\lambda$ and $\hat{\Omega}_\lambda \neq \hat{\Sigma}_\lambda^{-1}$.
2. There is no guarantee that $\hat{\Omega}_\lambda$ has real positive eigenvalues. If it has negative or complex eigenvalues, many multivariate procedures such as LDA and PCA may not be well-defined.
3. There may be differences between the edge sets of the concentration graphs corresponding to the respective upper and lower halves of $\hat{\Omega}_\lambda$.

We examine the causes of the lack of symmetry in Section 3 and suggest possible remedies in Section 4.

3. Cause of Asymmetry in the Glasso Concentration Matrix Estimator

The glasso algorithm, taken directly from [Hastie et al. \(2009\)](#), is shown in Algorithm 1. For further details concerning the glasso and its convergence, see [Friedman et al. \(2008\)](#) and [Hastie et al. \(2009\)](#). In Algorithm 1, S is the sample covariance matrix, λ is the glasso penalty parameter, and W is a matrix on which the glasso iterates. In Step 2 of Algorithm 1, W_{11} refers to the submatrix of W without its j^{th} row and column, and s_{12} is the j^{th} column of the sample covariance matrix without the diagonal element s_{jj} . In Step 3 of Algorithm 1, $\hat{\theta}_{12}$ for a given j is the j^{th} column of the matrix Θ without Θ_{jj} . Upon termination of the algorithm, the current iterate W is set to $\hat{\Sigma}_\lambda$ and Θ is set to $\hat{\Omega}_\lambda$, and referred to as the glasso estimators.

Algorithm 1 The glasso, exactly as it appears on p. 636 of [Hastie et al. \(2009\)](#).

1. Initialize $\mathbf{W} = \mathbf{S} + \lambda \mathbf{I}$. The diagonal of \mathbf{W} remains unchanged in what follows.
 2. Repeat for $j = 1, 2, \dots, p, 1, 2, \dots, p, \dots$ until convergence:
 - (a) Partition the matrix \mathbf{W} into part 1: all but the j th row and column, and part 2: the j th row and column.
 - (b) Solve the estimating equations $\mathbf{W}_{11}\beta - s_{12} + \lambda \cdot \text{Sign}(\beta) = 0$ using the cyclical coordinate-descent algorithm (17.26) for the modified lasso.
 - (c) Update $w_{12} = \mathbf{W}_{11}\hat{\beta}$
 3. In the final cycle (for each j) solve for $\hat{\theta}_{12} = -\hat{\beta} \cdot \hat{\theta}_{22}$, with $1/\hat{\theta}_{22} = w_{22} - w_{12}^T \hat{\beta}$.
-

3.1. Construction of $\hat{\Omega}_\lambda$ in the glasso

The glasso iteratively updates a matrix W which converges numerically to $\hat{\Sigma}_\lambda$, the glasso estimator for the population covariance matrix Σ . In contrast, the estimator $\hat{\Omega}_\lambda$ for the precision matrix Ω is constructed only upon convergence, i.e., only after the algorithm terminates. As we shall show below, the process by which $\hat{\Omega}_\lambda$ is constructed avoids inversion but is however mathematically inexact in the sense that it leads to $\hat{\Omega}_\lambda^T \neq \hat{\Omega}_\lambda$ and $\hat{\Omega}_\lambda^{-1} \neq \hat{\Sigma}_\lambda$. If $\hat{\Omega}_\lambda^T \neq \hat{\Omega}_\lambda$, the graph encoded by the glasso output $\hat{\Omega}_\lambda$ may be different from the graph encoded by $\hat{\Sigma}_\lambda^{-1}$. This problem was illustrated in the two motivating examples above.

Step 2 of Algorithm 1 involves an inner loop in which row/column $1, \dots, p$ of W are sequentially updated. For one full inner loop over the p rows and columns of W , let the p successive estimates be denoted $W^{(i)}$ for $i = 1, \dots, p$. Exactly one row and column of $W^{(i)}$ is updated using a lasso coefficient $\hat{\beta}^{(i)}$ ($\hat{\beta}$ of Step 2 in Algorithm 1).

We now introduce additional notation in order to illustrate the problems encountered when the glasso constructs an estimate of the concentration matrix (recall that this takes place upon termination of the glasso algorithm). Consider once more $W^{(i)}$ for $i = 1, \dots, p$. Define $\Theta^{(i)} \triangleq (W^{(i)})^{-1}$ and $\theta_{-i,i}^{(i)}$ to be the $(p-1)$ vector consisting of the i^{th} column of $\Theta^{(i)}$ excluding the diagonal entry $\theta_{ii}^{(i)}$. Define $w_{-i,i}^{(i)}$ and $w_{ii}^{(i)}$ be the corresponding elements of $W^{(i)}$ and let $W_{-i,-i}^{(i)}$ be the i^{th} principal minor of $W^{(i)}$. Then using the fact that $\Theta^{(i)} \triangleq (W^{(i)})^{-1}$, there is a closed-form expression for $\theta_{ii}^{(i)}$ and $\theta_{-i,i}^{(i)}$ in terms of s_{ii} , $w_{-i,i}^{(i)}$, and $\hat{\beta}^{(i)}$:

$$\theta_{-i,i}^{(i)} = -\hat{\beta}^{(i)}\theta_{ii}^{(i)}, \quad \theta_{ii}^{(i)} = \frac{1}{w_{ii}^{(i)} - (w_{-i,i}^{(i)})^T \hat{\beta}^{(i)}}. \quad (2)$$

When the glasso terminates, it sets $\hat{\Sigma}_\lambda = W^{(p)}$ and uses (2) to compute $\{\theta_{ii}^{(i)}, \theta_{-i,i}^{(i)}\}_{i=1}^p$, which are taken as the columns of $\hat{\Omega}_\lambda$. This procedure has a complexity of $\mathcal{O}(p^2)$ and is therefore more efficient than direct numerical inversion.

3.2. Cause of asymmetry in $\hat{\Omega}_\lambda$

The glasso terminates when W converges numerically, and constructs $\hat{\Omega}_\lambda$ from $\{\theta_{-i,i}^{(i)}, \theta_{ii}^{(i)}\}_{i=1}^p$. These are easily obtainable from previous iterations of the inner loop, thus avoiding the need to invert $W^{(p)}$. However, while $\{\theta_{-p,p}^{(p)}, \theta_{pp}^{(p)}\}$ is equal to the p^{th} row and column of $\Theta^{(p)} = (W^{(p)})^{-1} \triangleq \hat{\Sigma}_\lambda^{-1}$ by construction, the $\{\theta_{ii}^{(i)}, \theta_{i,-i}^{(i)}\}_{i=1}^{p-1}$ are not equal to the i^{th} row and column of $(W^{(p)})^{-1}$. Instead, by construction each $\{\theta_{ii}^{(i)}, \theta_{i,-i}^{(i)}\}_{i=1}^{p-1}$ is equal to the i^{th} row and column of $(W^{(i)})^{-1} \neq (W^{(p)})^{-1}$. Asymmetry occurs because the quantities $\{\theta_{ii}^{(i)}, \theta_{i,-i}^{(i)}\}_{i=1}^p$ are taken as the columns of $\hat{\Omega}_\lambda$.

The discrepancy between the above set of estimates may not be minimal even if the iterates $W^{(i)}$ are approximately equal. Another way of stating this problem is that convergence of the $W^{(i)}$ to a specified tolerance does not necessarily imply

convergence of $(W^{(i)})^{-1}$ to any given tolerance. The result is that while the glasso covariance estimator $\hat{\Sigma}_\lambda$ satisfies (1), $\hat{\Omega}_\lambda$ does not, leading to the aforementioned problems. The problem is exacerbated when the penalty parameter λ is small and S is close to rank-deficient (which is the case when $n \ll p$). The following lemma formalizes this assertion.

Lemma 1. *If S is rank-deficient, the maximum absolute value of the entries of $\hat{\Omega}_\lambda$ diverges as $\lambda \rightarrow 0$.*

Proof. See the appendix. □

Lemma (1) suggests that convergence of the inverse glasso iterates W^{-1} to some small, fixed tolerance may require a radically small tolerance criterion for the convergence of the glasso iterates W . Indeed, it is easy to construct such examples. Consider the rank-deficient sample covariance matrix S shown below alongside the optimal solution to (1) corresponding to a regularization parameter of $\lambda = 10^{-6}$:

$$S = \begin{bmatrix} 1 & 0 \\ 0 & 0 \end{bmatrix}, \quad \hat{\Sigma}_\lambda = \begin{bmatrix} 1 + 10^{-6} & 0 \\ 0 & 10^{-6} \end{bmatrix}, \quad \hat{\Omega}_\lambda = \begin{bmatrix} (1 + 10^{-6})^{-1} & 0 \\ 0 & 10^6 \end{bmatrix}. \quad (3)$$

Moreover, consider a matrix iterate W_t which is close to $\hat{\Sigma}_\lambda$, given as follows

$$W_t = \begin{bmatrix} 1 + 10^{-6} & 0 \\ 0 & (1 + t^{-1}) \times 10^{-6} \end{bmatrix}. \quad (4)$$

The supremum-norm errors on the dual and primal for this W_t are given respectively by

$$\|W_t - \hat{\Sigma}_\lambda\|_\infty = t^{-1}10^{-6} \quad \text{and} \quad \|W_t^{-1} - \hat{\Omega}_\lambda\|_\infty = \frac{1}{t+1}10^6, \quad (5)$$

and are several orders of magnitude apart. This example demonstrates why decreasing the convergence tolerance on the dual iterates W may not always be a feasible solution to the asymmetry problem discussed here.

To summarize, the method for inversion used during the final step of the glasso algorithm for computing $\hat{\Omega}_\lambda$ is mathematically inexact, and the resulting error is exacerbated when $p > n$ with an insufficiently large penalty parameter λ . In this case, the ℓ_1 -penalized inverse covariance estimator is unreliable as $\lambda \rightarrow 0$, as described by Lemma 1. Therefore the use of an overly small λ should be avoided; however, in practice, choosing the penalty parameter λ can be challenging. For example, choosing λ via cross-validation using $\hat{\Omega}_\lambda$ tends to yield overly small λ , which may produce dense and possibly ill-conditioned estimates for $\hat{\Omega}_\lambda$. One possible indicator of too little regularization is when the number of neighbors of each variable/node is too high. A second possible indicator is if there is a serious lack of symmetry in the glasso estimates. A third possible indicator is when the condition number of the resulting estimate is too high. Recently, [Won et al. \(2012\)](#) provide impetus for constraining the condition number of the covariance matrix; in light of that work, the condition number can perhaps be used as a guide in choosing λ .

4. Enforcing Symmetry on the Glasso Concentration Matrix Estimator

The glasso covariance estimator $\hat{\Sigma}_\lambda$ is the true numeric minimum of the glasso problem (1) and thus a valid ℓ_1 regularized estimator for the true population covariance matrix Σ . However, as previously demonstrated, the glasso estimator $\hat{\Omega}_\lambda$ is asymmetric, and $\hat{\Omega}_\lambda^{-1} \neq \hat{\Sigma}_\lambda$.

In some settings, it may be desirable to resolve one or both of the aforementioned issues. For $\hat{\Omega}_\lambda$ to encode a sparse concentration graph, its sparsity pattern must be symmetric. Moreover, if $\hat{\Omega}_\lambda$ is to be used as a sparse concentration matrix estimator, it is necessary that $\hat{\Omega}_\lambda^T = \hat{\Omega}_\lambda$ for it to be a valid estimator. Most importantly, it may be required that $\hat{\Omega}_\lambda = \hat{\Sigma}_\lambda^{-1} \succ 0$ in order for it to be usable in multivariate procedures.

We propose three simple approaches which address some or all of the above requirements.

1. **Numerical inversion.** To have $\hat{\Omega}_\lambda = \hat{\Sigma}_\lambda^{-1}$, it is necessary to directly invert $\hat{\Sigma}_\lambda$. This inversion maintains the sparsity pattern of $\hat{\Omega}_\lambda$ (although as a consequence of numerical error there may be negligible entries in place of zeroes). The $\mathcal{O}(p^3)$ complexity of numerical inversion (vs. $\mathcal{O}(p^2)$ for the current glasso approach) does not represent a difficulty for matrices of the dimension which the glasso is currently able to solve (up to $p \approx 2000$ on a typical desktop), as it also needs to be done only once at the end of the glasso iteration. Note that the inverted matrix $\hat{\Sigma}_\lambda^{-1}$ should be hard thresholded to eliminate small non-zero entries introduced by numerical error, and the resulting inverse covariance matrix then should be checked for positive definiteness. However, numerical inversion may not be a viable option when $\hat{\Sigma}_\lambda$ is ill-conditioned, as is the case when S is rank-deficient and λ is small. In such cases, it may be useful to exercise caution when using $\hat{\Omega}_\lambda$ in further calculations.
2. **Modified glasso output.** The upper right triangle of $\hat{\Omega}_\lambda$ can be taken as the correct estimate. The entries corresponding to the upper right triangle are more recent updates than those in the lower left triangle, since the glasso inserts the $\left\{ \theta_{-i,i}^{(i)}, \theta_{ii}^{(i)} \right\}_{i=1}^p$ into the columns of $\hat{\Omega}_\lambda$. The resulting estimator will not equal $\hat{\Sigma}_\lambda^{-1}$, but it is symmetric. It will not solve the primal problem in (1) exactly.
3. **Iterative proportional fitting (IPF).** IPF (Speed and Kiiveri, 1986) can be used to simultaneously compute the maximum likelihood estimates for Ω and Σ under an assumed concentration graph, i.e., sparsity pattern in $\hat{\Omega}$. One approach is to use the sparsity pattern from the upper right triangle of $\hat{\Omega}_\lambda$, enforce symmetry, and then use IPF to obtain $\hat{\Sigma}$ and $\hat{\Omega}$. The estimator $\hat{\Omega}$ will reflect the sparsity structure corresponding to $\hat{\Omega}_\lambda$, and satisfy $\hat{\Omega} = \hat{\Sigma}^{-1}$ at each iteration of IPF. Note that neither $\hat{\Omega}$ nor $\hat{\Sigma}$ will be solutions to (1) or (6), respectively. Furthermore, the computational complexity of IPF is $\mathcal{O}(c^3)$, where c is the size of the largest maximal clique of the graph implied by $\hat{\Omega}_\lambda$. Therefore, IPF does not imply relatively higher computational costs, although it does require identifying the maximal cliques which is well-known to be NP-complete. Finding the maximal cliques can however be avoided if a modification of the glasso algorithm is used to estimate an

undirected Gaussian graphical model with known structure (see Algorithm 17.1 in [Hastie et al. \(2009\)](#)).

Table 1 summarizes the properties and tradeoffs of each of the proposed solutions.

Table 1: Comparison of possible estimators.

Method	$\hat{\Omega}^T = \hat{\Omega}$	Latest updates in $\hat{\Omega}$	$\hat{\Omega} = \hat{\Sigma}^{-1}$	$\hat{\Sigma}$ solves (6)	$\hat{\Omega}$ solves (1)
Glasso Output	X	X	X	✓	X
Modified Output	✓	✓	X	✓	X
Numerical Inversion	✓	✓	✓	✓	✓
IPF	✓	X	✓	X	X

5. Conclusions

In this note we demonstrated that the estimators from the widely used R package *glasso* may be asymmetric when the amount of regularization applied is small. This could cause problems when the glasso estimators are used as inputs to other multivariate procedures, and additionally because the sparsity structure of the glasso estimators may themselves be asymmetric. It may be helpful for users of the package *glasso* to be aware of this, as the estimator can be easily corrected by one of the outlined methods. Of these, numerical inversion followed by thresholding may be the simplest and most effective fix. The root cause of the issue is that the glasso algorithm operates on the dual of (1), and constructs the primal estimator, $\hat{\Omega}_\lambda$, only after the dual optimization completes. If a sparse concentration estimator is sought, it may be more natural to operate off the primal problem (1), though the glasso is more popular in practice. Methods for solving the primal (1) have been recently considered, among others see [Maleki et al. \(2010\)](#) and [Mazumder and Agarwal \(2011\)](#). This short note avoids recourse to the primal by identifying problems with the dual approach, and consequently explores ways in which these can be easily rectified so that the popular dual approach can be retained.

Acknowledgments

We acknowledge Trevor Hastie and Robert Tibshirani (Department of Statistics, Stanford University) for discussions.

Benjamin Rolfs was supported in part by the Department of Energy Office of Science Graduate Fellowship Program DE-AC05-06OR23100 (ARRA) and NSF grant AGS1003823. Bala Rajaratnam was supported in part by NSF grants DMS0906392 (ARRA), AGS1003823, DMS (CMG) 1025465, DMS1106642 and grants NSA H98230-11-1-0194, DARPA-YFA N66001-11-1-4131 and SUFSC10-SUSHSTF09-SMSCVISG0906.

References

Banerjee, O., El Ghaoui, L., d’Aspremont, A., 2008. Model selection through sparse maximum likelihood estimation for multivariate gaussian or binary data. *Journal of Machine Learning Research* 9, 485–516.

- Friedman, J., Hastie, T., Tibshirani, R., 2008. Sparse inverse covariance estimation with the graphical lasso. *Biostatistics* 9, 432–441.
- Hastie, T., Tibshirani, R., Friedman, J., 2009. *Elements of Statistical Learning*. Springer, New York. 2nd edition.
- Maleki, A., Rajaratnam, B., Wong, I., 2010. Fast iterative thresholding algorithms for sparse inverse covariance Selection. Technical Report.
- Mazumder, R., Agarwal, D.K., 2011. A flexible, scalable and efficient algorithmic framework for the *Primal* graphical lasso. Pre-print [arXiv:1110.5508v1](https://arxiv.org/abs/1110.5508v1).
- Speed, T., Kiiveri, H., 1986. Gaussian markov distributions over finite graphs. *Annals of Statistics* 14, 138–150.
- Won, J., Lim, J., Kim, S., Rajaratnam, B., 2012. Condition number regularized covariance estimation. *Journal of the Royal Statistical Society Series B* (in press) .

Appendix

Proof. Consider the dual of (1) as given in [Banerjee et al. \(2008\)](#):

$$\begin{aligned} \hat{\Sigma}_\lambda &= \arg \min_{X \succ 0} [\log \det (X)] \\ \text{s.t. } &\max_{i,j} |x_{ij} - s_{ij}| \leq \lambda \end{aligned} \tag{6}$$

where $\max_{i,j} |m_{ij}|$ is the supremum norm, the maximum absolute value entry of the matrix M . From (6), it is clear that $\hat{\Sigma}_\lambda \rightarrow S$ in the supremum norm as $\lambda \rightarrow 0$, though at $\lambda = 0$ the primal problem (1) does not necessarily have a solution. Convergence in sup-norm gives convergence of $\hat{\Sigma}_\lambda \rightarrow S$ in any other operator norm $\|\bullet\|_*$. In particular, invoking the continuity of eigenvalues, $\lambda_{\min}(\hat{\Sigma}_\lambda) \rightarrow \lambda_{\min}(S)$ as $\lambda \rightarrow 0$, with $\lambda_{\min}(M)$ defined as the smallest eigenvalue of the square matrix M . Considering the operator 2-norm and ∞ -norm of $\hat{\Sigma}_\lambda^{-1}$ gives:

$$\begin{aligned} \max_{i,j} \left| \left(\hat{\Omega}_\lambda \right)_{ij} \right| &= \max_{i,j} \left| \left(\hat{\Sigma}_\lambda^{-1} \right)_{ij} \right| \\ &\geq p^{-1} \left\| \hat{\Sigma}_\lambda^{-1} \right\|_\infty \\ &\geq p^{-1} \left\| \hat{\Sigma}_\lambda^{-1} \right\|_2 \\ &= p^{-1} \lambda_{\max} \left(\hat{\Sigma}_\lambda^{-1} \right) \\ &= p^{-1} \left[\lambda_{\min} \left(\hat{\Sigma}_\lambda \right) \right]^{-1} \\ &\xrightarrow{\lambda \rightarrow 0} p^{-1} \left[\lambda_{\min} (S) \right]^{-1} \end{aligned}$$

In the sample-deficient case $n \ll p$, $\lambda_{\min}(S) = 0$ almost surely, and therefore $\hat{\Omega}_\lambda$ diverges with respect to the supremum norm as $\lambda \rightarrow 0$. \square